Rev. Roum. Sci. Techn.– Électrotechn. et Énerg.
Vol. **65**, *1-2*, pp. 145–150, Bucarest, 2020

Dedicated to the memory of Academician Gleb Drăgan

ANALYSIS OF MAGNETOTHERAPY EFFECTS FOR POST–TRAUMATIC RECOVERY OF LIMB FRACTURES

ROXANA-MARIA BAEROV[1], ALEXANDRU-MIHAIL MOREGA[2,3], MIHAELA MOREGA[2]

Keywords: **Magnetotherapy, Medical images based computational domain, Magnetic field, Heat transfer, Numerical simulation, Finite element method.**

Magnetotherapy is one of the most popular methods of physiotherapy and is used in orthopedics, rheumatology or for the treatment of internal diseases. The success of magnetotherapy could be improved provided that non-invasive post-interventional evaluation of its effects is performed with the aid numerical modeling. In order to provide meaningful insights, the evaluation has to be patient–related, and to this aim tailored computational domains are needed. This study is concerned with the numerical modeling of the magnetic field problem associated to magnetotherapy and possible side effects due to electromagnetic heating of metallic orthopedic implants, using two computational stages: a simplified one, approach, with the computational domain built from geometric shapes and a complex and more realistic one, with the computational domain built using medical images based techniques.

1. INTRODUCTION

Due to severe trauma limb long bones can be fractured and the healing requires long periods of time with imobilization and disconfort for the patient. The main causes of limb fractures are major impacts on the bone, such as traffic accidents, falls, but also if the person suffers from a pre-existing bone disease. Highest incidence occurs in young people due to sporty dynamic life style and in older people (commonly over 70 years, due to bone fragility caused by osteoporosis and decreased agility).

The study presented here addresses the fracture of long bones and applies to the largest and strongest bone in the lower extremity of the human body, the femur. In particular, this bone can be fractured in three areas: the head / neck of the bone (upper end), the diaphysis (midsection), or near the knee (lower end). Simple fractures (small cracks in the bone) do not require surgery, but in general the treatment is surgical and aims to stabilize the fractured bone with metallic structures. In case of severe femoral fractures, an intramedullary rod is inserted in the center of the femoral bone and it is fixed with screws. Other alternatives to fix the femur are the use of plate and screws outside the bone or an external fixator [1,2].

Post surgical healing of soft tissues and natural repair of bone require immobilization, which quickly leads to reduction in muscle volume and strength, loss of physical fitness, or even musculoskeletal and neuronal disorders, with long and difficult recovery. For that reason, shortening the downtime and restoring mobility are very important and physiotherapy is helpful. One of the most popular methods of physiotherapy used succesfuly in orthopedics, but also in rheumatology or for the treatment of internal diseases is magnetotherapy. Among the main benefits of this method are pain relief and a shortened healing time for the fractured bone tissue. Magnetotherapy has a significant effect on trophic stimulation of bones and collagen by producing microcurrents that accelerate osteogenesis [3–10].

The paper aims to study the the magnetic field problem associated to magnetotherapy and possible side effects due to electromagnetic heating of metallic orthopedic implants, using a simple, three-dimensional computational domain that reproduces the bone and the tissue, as well as a complex calculation domain obtained by imaging reconstruction.

2. MAGNETOTHERAPY

In ancient times, physicians used natural magnetic materials to treat certain diseases. This approach was later used in China, Japan and Europe. Between 1960 and 1985, most European countries had designed and manufactured magnetotherapeutic systems that used different waveforms [5]. Magnetotherapy is one of the basic physiotherapy procedures. The initial technique was to apply a static magnetic field on the area that needs to be healed. The rapid development of low-frequency pulsed magnetotherapy has led to the conclusion that time-variable magnetic field is dozens of times more effective than static magnetic field for various therapies. In addition, it can be used in combination with other methods of therapy, such as pharmacotherapy. The physiological response of the body to the application of magnetotherapy involves multiple effects: analgesic, antiedematous, trophic (acceleration of healing by growth), vasodilation and muscle relaxation [11].

Theraputic protocols are generally set on empirical basis, but magnetotherapy has already gain the recognition in the medical world, for significant benefits brought to people suffering from musculoskeletal disorders, injuries or pain. In addition, musculoskeletal disorders related to bone fractures and chronic injuries, but also diseases such as Parkinson or Alzheimer are other applications that magnetotherapy could bring benefits for. Magnetotherapy improves the process called osteogenesis, helping to accelerate wounds and fractures healing. In addition, magnetotherapy has been shown to improve the biomechanical properties of a diabetic bone. When the conventional treatment does not produce proper results, magnetotherapy can provide benefits such as: reduced pain, costs and duration of treatment [5,13,14].

Magnetotherapy is based on the fundamental principle of

[1] University "Politehnica" of Bucharest, Faculty of Medical Engineering, Bucharest, Romania
[2] University "Politehnica" of Bucharest, Faculty of Electrical Engineering, Bucharest, Romania
[3] "Gh. Mihoc – C. Iacob" Institute of Statistical Mathematics and Applied Mathematics, Romanian Academy, Bucharest, Romania
Corresponding author: alexandru.morega@upb.ro

electromagnetic induction. A time-varying electric current passing through a coil placed on the anatomical region creates a time-varying magnetic field. This magnetic field produces an electric field in that tissue that depends on the characteristics of the applied magnetic field and the properties of the tissue [11].

The magnetic field used for magnetotherapy can be static, alternating or pulsating [11]. In general, magnetotherapy is characterized by low frequencies in the range of 10–100 Hz (sometimes even up to 170 Hz). In order to obtain an effective result for certain diseases, it is advisable to use only certain waveforms [13]:

- sinusoidal waveforms – used in applications related to nerves or muscles distortion;
- pulse waveforms – used for bone diseases;
- triangular waveforms – used in applications related to cartilages or tendons dysfunctions.

Continuous magnetotherapy is advisable in circumstances when the effects of the pulse electromagnetic field could produce serious harms, *e.g.*, in case of increased bleeding conditions, acute states, post-operative conditions, *etc*. The effect of this type of stimulation is also augmented by permanent magnets embedded within the "disc" type applicators [11,12]. This type of field is recommended in the first stages of magnetotherapy. After the couple of weeks it is recommended to change over to the pulse field. Continuous magnetic field can be modulated by slow magnetic field surges with a length of several seconds or more: sine, trapezoid, and symmetric surges.

The coils used for magnetotherapy should be placed as close as possible to the patient's body, for the minimization of dispersive magnetic flux. The minimum exposure time is at least 10 minutes, and the total daily exposure should not exceed 40 minutes. For best results exposures should be made repeatedly [11].

Numerical modeling has recently gained in importance and recognition for medical therapy assistance, both for pre-interventional assessment and for the evaluation of response to medical treatment or post-interventional evolution. We present here the design of a computational model that represents the anatomy of the upper leg (first as a simplified and than as a realistical anatomy structure) exposed to variable magnetic field, generated by an induction coil; the magnetic field problem associated to magnetotherapy is solved by numerical analysis, with the finite element method (FEM). In an advanced stage of the study, the metallic structure of an orthopedic implanted device is considered as the target of eddy currents and the associated thermal effect is assessed too.

3. IMAGING RECONSTRUCTION

Initially, the simulations were performed using a simplified 3D computational domain. To make the model as similar as possible to human anatomy, the tissue was built as a cylinder; inside it is another cylinder that represents the femur. A platinum plate, built as a 170 mm long parallelepiped, is placed on the femur. The computational domain is limited to a section of the leg surrounded by air and bounded by a cylindrical surface and two short cylindrical infinite domains (top and bottom). The magnetic field is generated by two induction coils, placed on the sides of the femur-like cylinder.

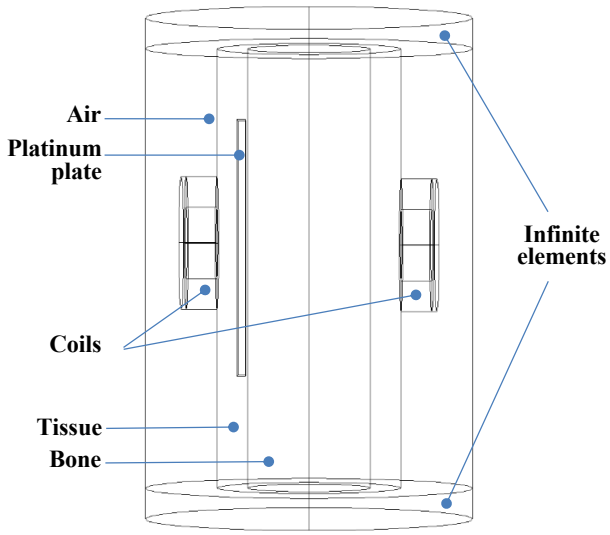

Fig. 1 – Simplified computational domain. Infinite elements are used to close it within a conveniently limited volume.

A realistic model is essential to achieve reliable results for medical applications, in general, and can be used for numerical modeling and simulations in various problems too, while enhancing the diagnosis accuracy.

3D Slicer [15] was further used for imaging reconstruction in an attempt to create an anatomically realistic computational domain. This open source software uses as input computed tomography (CT) images in axial, coronal, and sagittal planes to create a three–dimensional model. The image set "Femur 1.0.0" was taken from [16]. The final model must contain the femur and the surrounding tissue.

The first step was to create a three-dimensional model for bone and surrounding tissue, as seen in Figs. 2 and 3.

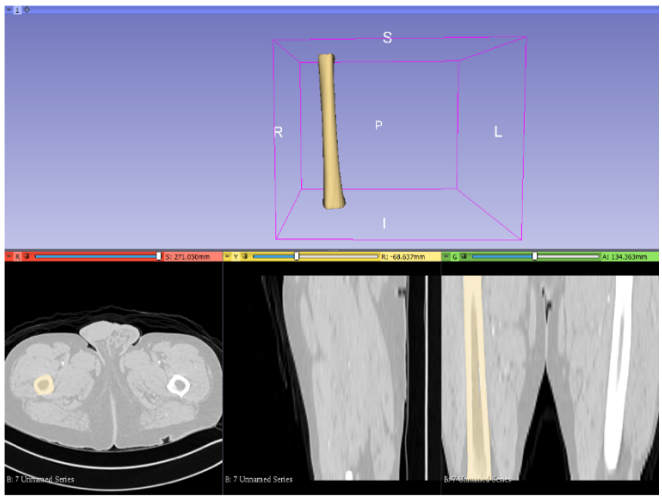

Fig. 2 – Femur 3D model obtained in 3D Slicer.

The next step was to import into MeshLab [17] each model created in 3D Slicer for processing and reducing its complexity (Fig. 4). In this open source software, some unwanted regions were eliminated. Then the *Quadric Edge Collapse Decimation* function was used to reduce the complexity of the model. This is especially relevant for high–resolution 3D models because in this way the computational time can be reduced. In the end, two domains were obtained.

Models processed in MeshLab are saved in 3DS format.

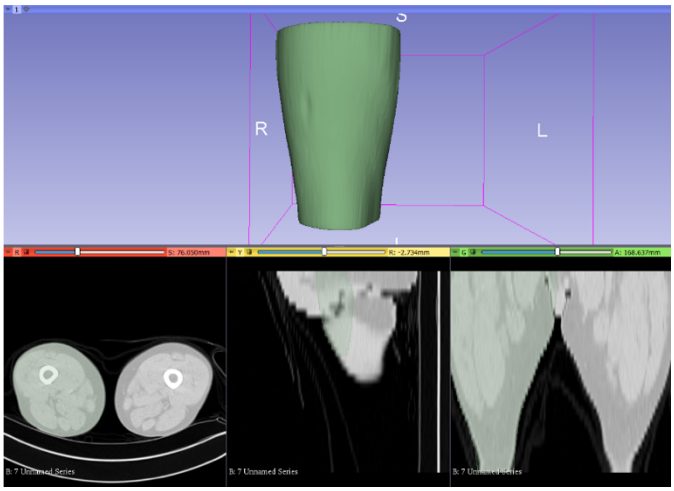

Fig. 3 – Tissue 3D model obtained in 3D Slicer.

Using AutoCAD [18], the models were converted to 3D Solid entities using *MESHOPTIONS* and *CONVTOSOLID* commands. The final step consists of assembling all the previously created models. The final model was saved in IGES format to be compatible with the FEM solver [19].

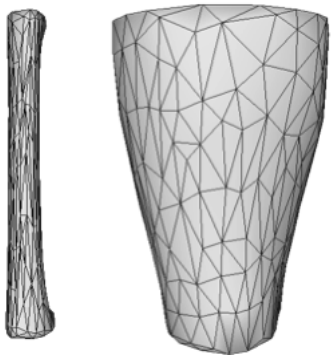

Fig. 4 – The two models processed using Meshlab.

After the 3D Slicer imaging reconstruction was performed, the two cylinders representing the tissue and the femur (in Fig. 1) were replaced with the three-dimensional models in order to obtain a computational domain as close to reality as possible (Fig. 5).

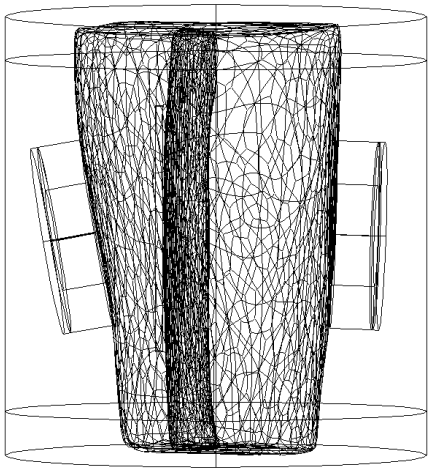

Fig. 5 – Computational domain obtained by imaging reconstruction. Lagrange quadratic elements are used for the FEM mesh (approx. 240,000).

4. NUMERICAL MODELS

In this study, two problems are modeled: Magnetic Field and Heat Transfer.

4.1. PHYSICAL AND MATHEMATICAL MODEL

For the magnetic field problem a time-harmonic operating mode is used. The equations that describe the problem are

$$\nabla \times \underline{\mathbf{H}} = \underline{\mathbf{J}} \tag{1}$$

$$\underline{\mathbf{J}} = \sigma \underline{\mathbf{E}} + \mathrm{j}\omega \underline{\mathbf{D}} + \underline{\mathbf{J}}_e, \tag{2}$$

$$\underline{\mathbf{B}} = \nabla \times \underline{\mathbf{A}}, \tag{3}$$

$$\underline{\mathbf{E}} = -\mathrm{j}\omega \underline{\mathbf{A}}. \tag{4}$$

The complex images of physical quantities are underscored, $\mathrm{j} = \sqrt{-1}$, $\omega = 2\pi f$ is the angular frequency and f is the frequency. In equations (1) – (4), $\underline{\mathbf{H}}$ [A/m] is the magnetic field strength, $\underline{\mathbf{J}}$ [A/m^2] is electric current density, $\underline{\mathbf{B}}$ [T] is the magnetic flux density, $\underline{\mathbf{A}}$ is the vector potential, σ [S/m] is the electrical conductivity, $\underline{\mathbf{E}}$ [V/m] is the electric field strength, $\underline{\mathbf{D}}$ [C/m^2] is the electric flux density, and $\underline{\mathbf{J}}_e$ [A/m^2] is the externally generated current density.

The boundary condition applied to the air domain is magnetic insulation ($\mathbf{n} \times \underline{\mathbf{A}} = 0$).

In the simulation, two circular coils with a diameter of 130 mm are used and are placed on the surface of the tissue. Each coil is made of copper and consists of 200 turns. The coils are energized by a current source at 1 A. The currents passing through the two coils have opposite directions. To focus the magnetic field, an iron core was built inside the coil and a plate, which is composed of an alloy containing nickel, iron and molybdenum is placed behind the coil.

The electrical and magnetic properties are involved in the material laws: $\underline{\mathbf{B}} = \mu \underline{\mathbf{H}}$ and $\underline{\mathbf{D}} = \varepsilon \underline{\mathbf{E}}$, where μ [H/m] is the magnetic permeability and ε [F/m] is the electric permittivity of the respective material.

The electric and magnetic properties of the tissues are set based on the particular frequency of the electrical current that flows through the coils f = 100 Hz, Table 1 [20,21]. Because the femur is modeled as a single, equivalent domain (with equivalent properties), its electrical permittivity and electrical conductivity are calculated as mean values of the constituent anatomical regions: cortical bone, trabecular bone, and bone marrow. The tissue is similarly modeled, its constituent anatomical components are: skin, fat, muscle and blood.

Table 1

Electrical properties of the tissues at 100 Hz

Tissue type	ε [F/m]	σ [S/m]
Femur	8.7×10^{-7}	5.08×10^{-2}
Tissue	2.1×10^{-5}	0.25

For the heat transfer problem a transient analysis is used. The equations that describe the problem are

$$\rho C_p \frac{\partial T}{\partial t} + \nabla \cdot \mathbf{q} = Q + Q_{met}, \tag{5}$$

$$\mathbf{q} = -k \nabla T. \tag{6}$$

In equations (5)–(6), ρ [kg/m^3] is the density of the tissue, C_p [J/(kg·K)] is the specific heat at constant pressure of the

tissue, T [K] is the temperature of the tissue, $\mathbf{q}$ [W/m^2] is the heat flux, Q [W/m^3] is the heat source, Q_{met} [W/m^3] is the metabolic heat source (which is neglected in this study) and k [W/(m·K)] is the thermal conductivity of the tissue. The heat source Q is taken from the magnetic field problem by volumetric loss density.

The boundary condition that closes the model is

$$q_0 = h(T_{ext} - T), \tag{7}$$

where q_0 [W/m^2] is the inward heat flux, h is the heat transfer coefficient (set to 2 W/(m^2·K), and T_{ext} is the external temperature (set to 20°C). The pressure is 1 atm. The initial tissue temperature is 37°C.

The thermal properties of the two tissues (Table 2) are taken from [22]. Again, the femur and tissue are modeled as equivalent, homogeneous, not perfuse domains, the thermal properties for each calculated as mean values of the constituent anatomical regions.

Table 2

Thermal properties of the tissues

Tissue type	*Cp* [J/kg·K]	ρ [kg/m^3]	*k* [W/m·K]
Femur	2080	1273	0.27
Tissue	3195	1040	0.40

The mathematical model (1) – (4) is solved numerically, using Galerkin FEM [19] – linear vector elements for the magnetic field and cubic Lagrange elements for the heat transfer. First the electromagnetic field is solved for using PARDISO direct solver [23]. Using the power density thus calculated, the non-stationary heat transfer problem (5) – (7) is then integrated, using MUMPS solver [24].

5. **RESULTS**

For the characteristics of the source established here (the current fixed through the coils at the frequency of 100 Hz), the magnetic flux density reaches the maximum value of 60 mT in the centers of the coils. Our study seeks to assess some technical characteristics of the megnetotherapy procedure and to identify the risks of side effects, if any.

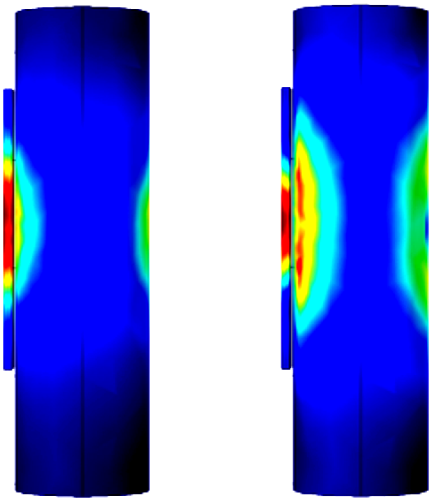

Fig. 6 – Magnetic flux density (left) and electric field strength (right) in the femur with fixation plate; magnetic field concentrators are attached to the coils.

Three cases are thus analysed and discussed: (1) the more complex model includes magnetic field concentrators attached to the inductive coils, which are placed by the sides of the thigh and a metallic, high conductive, orthopedic implant fixed on the femural bone; (2) simple coils (without magnetic concentrators) are considered as applicators for the same bone with attached implant; (3) the coils with attached magnetic concentrators apply the magnetic field to the leg without including the conductive implant.In the first case, the maximum value of the magnetic flux density at the level of the fixation plate is 40 mT (Fig. 6, left), while in the bone tissue the maximum value 20 mT. Figure 6 (right) shows the electric field strength and it is observed that there are local maxima close to the regions where the coils are placed, where a higher current density is expected to occur. The maximum value of the electric field strength inside the bone is 0.4 V/m.

Figure 7 shows the color maps of the magnetic flux density and the electric field strength when the coil is simple, without the materials (iron core and plate behind the coil) that concentrate the magnetic field on the target volume. The maximum value of the magnetic flux density is 20 mT at the implant, and a respective peak value of 10 mT inside the bone. The maximum value of the electric field strength is 0.24 V/m. All these values are lower than those obtained for coils without concentrators, showing that coils with magnetic concentrators can be more efficient for the performed treatment.

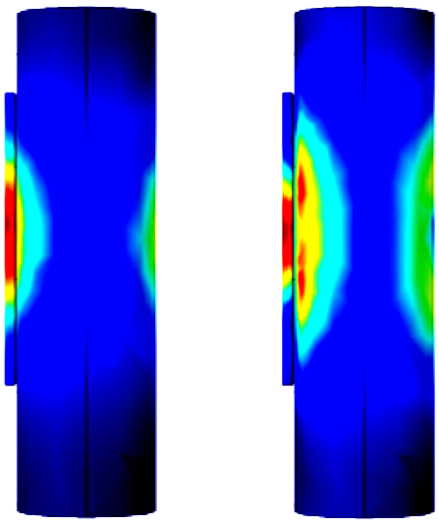

Fig. 7 – Magnetic flux density (left) and electric field strength in the femur (right) for coils without magnetic concentrators.

Figure 8 shows the values of the magnetic flux density and the electric field strength for the bone without fixation plate, when applicators with magnetic field concentrators are used. The maximum value of the magnetic flux density inside the bone tissue is 30 mT, while the maximum value of the electric field strength is 0.28 V/m.

The values of the electric field inside the bone are lower than those obtained with fixation plate. The plate is made of platinum; a metallic material with high conductive properties was selected considering the maximization of the heating potential due to the eddy currents induced in the fixing plate during magnetotherapy.

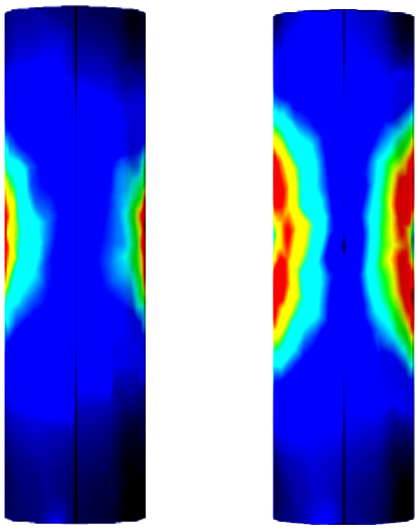

Fig. 8 – Magnetic flux density (left) and electric field strength (right) in the femur without fixation plate; magnetic field concentrators are attached to the coils.

In the absence of this plate, the fields reach directly into the bone tissue and extend over a larger area. So, the plate can influence the magnetotherapy procedure.

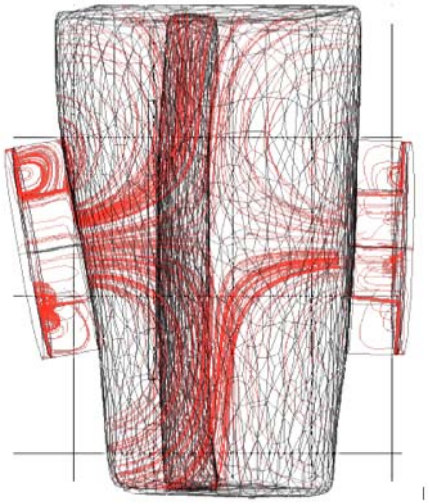

Fig. 9 – Magnetic flux density lines.

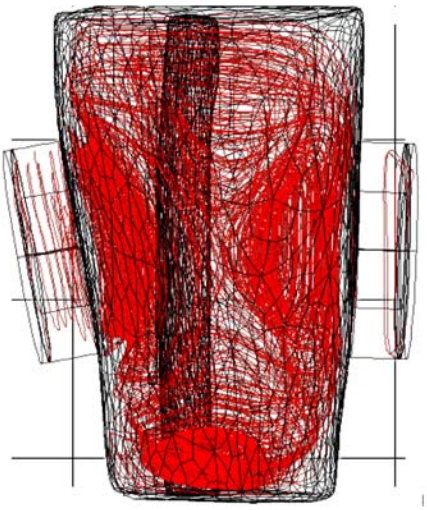

Fig. 10 – Electric field strength lines.

The distributions of magnetic flux density (Fig. 9) and electric field strength (Fig. 10) through the tissue were represented using the computational domain obtained by imaging reconstruction from CT images. The magnetic field (more concentrated near the coils), induces an electric field (solenoidal) in the tissues. The electric field reaches the region of the bone tissue that needs to be treated.

For the heat transfer problem, the heat source Q is taken from the magnetic field problem as the resistive heating (*i.e.*, volumetric loss density). Figure 11 illustrates, the resistive heating, which is located mainly in the highly conductive fixation plate.

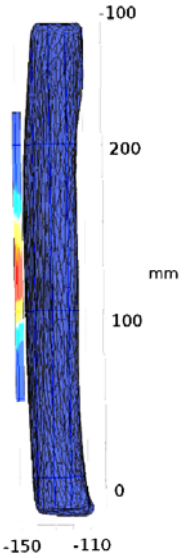

Fig. 11 – Specific heat losses – peak value 79.4 W/m^3.

Figure 12 demonstrates that the tissue temperature does not exceed 37°C after 15 minutes of exposure. The current carrying coils could heat up and in contact with the surface of the tissue can sometimes produce a mild heating of the skin, but this also depends on the frequency used for therapy. Low frequency magnetotherapy (for example 100 Hz) is not used in order to obtain a thermal effect, so it can be considered a useful and safe method for healing bone tissue even when there is an implant, a plate with screws or an external fixation.

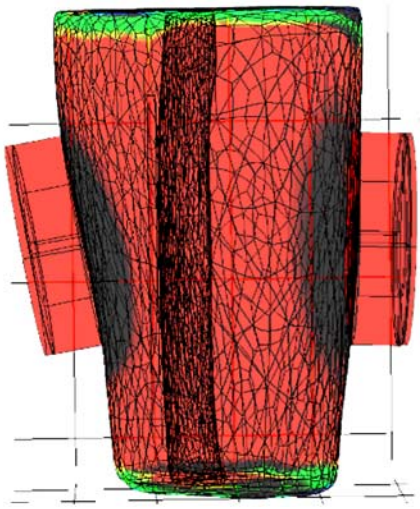

Fig. 12 – Quasi-uniform temperature after 15 min of magnetotherapy does not exceed 37°C.

CONCLUSIONS

For the pre–interventional, non–invasive evaluation of procedural features associated to magnetotherapy through numerical simulation to unveil meaningful insights, it has to be patient–specific, therefore tailored computational domains are at a prime. This study refers to the numerical modeling of magnetotherapy using a simple computational domain, built from geometric shapes, but also a complex one, built using medical images based techniques. The magnetic field and the electric field are calculated, and the results provide important information. The magnetic field and the electric field can be focused on the area that needs treatment using magnetic field concentrators (an iron core and a plate placed behind the coil).

Low frequency magnetotherapy does not cause thermal effects, so it can be considered a useful and safe method for healing bone tissue even when a conductive implant, like a plate with screws or an external fixator, was applied during the surgical intervention. The existence of an implant can influence the procedure in terms of **B** and **E** values that reach the bone tissue.

The complexity of the anatomic structure, the resolution and accuracy of the input CT images, on one hand, and the computational resources on the other hand led to a compromise in what concerns the scale of the details accounted for – the femur and the tissue are modeled as equivalent domains. More refined models make the object of a future research, as well as a CAD construction of the fixed plate or a femoral implant.

A future study will be concerned with simulating the effects of magnetotherapy using various waveforms. It is also desired to find the right frequency and the appropriate exposure time for each waveform applied, in order to obtain optimal results. Continuing the heat transfer study in terms of high frequency magnetotherapy is another future direction.

ACKNOWLEDGEMENTS

The study was conducted in the laboratory for Electrical Engineering in Medicine, the Faculty of Electrical Engineering.

Received on June 23, 2020

REFERENCES

1. ****Femur Fracture: Symptoms, Treatment, Recovery, Complications*, (in Romanian) https://www.reginamaria.ro/dictionar-de-afectiuni/fractura-de-femur — available in 2020.
2. ****Uptodate*. Uptodate.Com, https://www.uptodate.com/contents/midshaft-femur-fractures-in-adults — available in 2020.
3. E. Łada-Tondrya, *The impact of applicator size on distribution of electromagnetic field used in magnetotherapy*, Przeglad Elektrotechniczny, **1**, *7*, pp. 27–30 (2019).
4. ****The Value of The Magnetic Field In Bone Fractures*, Efisioterapia.Net, https://www.efisioterapia.net/en/the-value-of-the-magnetic-field-in-bone-fractures-t-7066.html — available in 2020.
5. M.S. Markov, *Expanding use of pulsed electromagnetic field therapies*, Electromagnetic Biol. and Med., **26**, *3*, pp. 257–274 (2007).
6. W. J.W. Sharrard, *A double-blind trial of pulsed electromagnetic fields for delayed union of tibial fractures*, J. Bone Joint Surg. [Br], **72,** *B*, pp. 347–355 (1990).
7. B. Chalidis, N. Sachinis, A. Assiotis, G. Maccauro, *Stimulation of bone formation and fracture healing with pulsed electromagnetic fields: biologic responses and clinical implications*, Int. J. Immunopathology and Pharmacology, **24**, *I* (*S2*), pp. 17–20 (2011).
8. H.-f. Shi, J. Xiong, Y.-x. Chen, J.-f. Wang, X.-sh. Qiu, Y.-h. Wang, Y. Qiu, *Early application of pulsed electromagnetic field in the treatment of postoperative delayed union of long-bone fractures: a prospective randomized controlled study*, *BMC Musculoskeletal Disorders*, **14**, *35*, pp. 7 (2103).
9. M.E. Moncada, C. Sarmiento, C. Martinez, A. Martinez, *Magnetic stimulation for fracture consolidation – clinical study*, 33rd Annual Int. Conf. of the IEEE EMBS, Aug. 30 – Sept. 3, 2011, Boston, MA, USA.
10. W. Pawluk, *Magnetic fields for pain control*, Electromagnetic Fields in Biology and Medicine, Ed. M.S. Markov, CRC Press, 2015.
11. ***BTL–4000 Magnetotherapy, User's guide, http://www.frankshospitalworkshop.com/equipment/documents/physiotherapy/user_manuals/BTL%20Magnetotherapy%204000%20-%20User%20manual.pdf — available in 2020.
12. E. Łada-Tondyra, *The impact of applicator size on distribution of electromagnetic field used in magnetotherapy*, Przegląd Elektrotechniczny, **95**, *7*, pp. 25–28 (2019).
13. A. Krawczy, P. Murawski, E, Korzeniewska, *Medical and technical analysis of magnetotherapeutical devices*, IEEE Int. Conf. on Modern Electrical and Energy Systems (MEES), 15–17 Nov. 2017, Kremenchuk, Ukraine.
14. B. Chalidis, N. Sachinis, A. Assiotis, G. Maccauro, *Stimulation of bone formation and fracture healing with pulsed electromagnetic fields: biologic responses and clinical implications*, Int. J. of Immunopath. and Pharm., **24**, *1*_suppl. 2, pp. 17–20 (2011).
15. ***3DSlicer, https://www.slicer.org/
16. ***Embodi3d.Com, https://www.embodi3d.com/files/file/33822-femur/ — available in 2020.
17. ***Meshlab, www.meshlab.net
18. ***Autocad, https://www.autodesk.com
19. ***Comsol Multiphysics, v.3.5a…5.3a.
20. C. Gabriel, *Compilation of the Dielectric Properties of Body Tissues at RF and Microwave Frequencies*, Report N.AL/OE-TR-1996-0037, Occupational and environmental health directorate, Radiofrequency Radiation Division, Brooks Air Force Base, Texas, USA (1996).
21. ****Dielectric Properties*, IT'IS Foundation, Itis.swiss, https://itis.swiss/virtual-population/tissue-properties/database/dielectric-properties/ — available in 2020.
22. ****Heat capacity*, IT'IS Foundation, Itis.swiss https://itis.swiss/virtual-population/tissue-properties/database/heat-capacity — available in 2020.
23. O. Schenk, K. Gartner, *Parallel Sparse Direct And Multi - Recursive Iterative Linear Solvers*, User Guide 6.0.0, https://pardiso-project.org/manual/manual.pdf (2018).
24. ****MUltifrontal Massively Parallel sparse direct Solver*, MUMPS Consortium, http://mumps.enseeiht.fr/ — available in 2020.